Influence of dimensionality and statistics on the Coulomb coupling between electron gases or electron-and-hole gases

Yu. M. Sirenko
Institute of Semiconductors, Academy of Sciences, 45 Pr. Nauky, Kiev, 252650, Ukraine

P. Vasilopoulos
Department of Physics, Concordia University, 1455 de Maisonneuve Boulevard West, Montréal, Québec, Canada H3G 1M8

(Received 16 January 1992)

Mutual Coulomb scattering between a one-dimensional electron gas (1DEG) and an i-dimensional electron gas ($i = 1, 2, 3$), separated by a finite distance ℓ, or a one-dimensional hole gas is considered. The gases can have the *same* or *different* statistics. The momentum and energy relaxation frequencies are evaluated using a drifted Fermi-Dirac distribution function and taking into account dynamical screening. For a *degenerate* 1DEG the main contribution to these frequencies comes from processes involving small momentum changes and backscattering. The screening of the first process can be significant even for a weakly nonideal 1DEG. The contribution of backscattering vanishes at large separations ℓ. The phase-space restrictions imposed by the conservation laws render the scattering rate between two *strongly degenerate* 1DEG's exponentially small everywhere except for narrow ranges of the concentrations. The dependences of the scattering rates on the temperature, the carrier concentrations, and the distance ℓ are evaluated analytically and numerically for a number of realistic cases.

I. INTRODUCTION

It has been predicted that momentum and energy transfer between spatially separated electron-gas layers, mediated by the Coulomb interaction, influences the transport properties of the individual layers.[1-3] This has been confirmed experimentally by the observation of a *contactless* current in a semibounded three-dimensional (3D) layer induced from that driven through another two-dimensional (2D) layer about 300 Å apart and vice versa.[4] Later on a similar experiment was carried out between two 2D gases but with no current allowed to flow in the second layer.[5,6] The experiment[6] demonstrated convincingly that an additional coupling mechanism, most clearly seen at large distances between the layers, was present.

Theoretical work pertinent to the first experiment was published in Refs. 7 and 8. The results of the second experiment have been explained theoretically in Ref. 9 by considering virtual-phonon exchange between the two layers in addition to the direct (screened) Coulomb coupling. Another work[10] considered the coupling, due to momentum transfer, between two one-dimensional (1D) gases in the presence of a perpendicular magnetic field.

Basic to all theoretical treatments are the concepts of energy and momentum transfer. To our knowledge both aspects have been treated only for the 2D-3D (Refs. 3 and 7) and 2D-2D (Ref. 11) coupling. Given the importance of quantum wires as potential devices, the importance of the effect, and the attention both have attracted, we feel that the coupling between separated electron gases deserves further studies. The purpose of this paper is to study the coupling between a 1D gas and a one-, two-, or three-dimensional gas, with the *same* or *different* statistics. The only pertinent work that we are aware of is Ref. 12 for two 1D or 2D gases of the same statistics. As expected and as will be shown the difference in dimensionality and statistics modifies considerably certain aspects of the coupling. The latter will be assumed to result only from the direct screened Coulomb interaction between the gases and any phonon mediated coupling[6,9] between the gases will be left out of consideration. The basic expressions for the relaxation frequencies are presented in Sec. II. In Sec. III they are evaluated analytically and in Sec. IV numerically. Remarks and conclusions follow Sec. V and the Appendixes give details about the relevant dielectric functions.

II. BASIC EXPRESSIONS

We consider a 1D electron gas (1DEG), along the x axis, coupled by Coulomb interaction with an i-dimensional gas, i = 1, 2, 3, and from which is separated by a distance ℓ as indicated in Fig. 1. In all cases we assume that the 1DEG occupies the lowest subband and that the thickness along the z axis is zero. Finite thickness and multisubband occupation can be taken into account in a straightforward manner.[13] The lattice dielectric constant is denoted by ϵ_L. For concreteness we further assume that the potential that confines the 1DEG along the y direction is parabolic, $V(y) = m_1^*\omega'^2y^2/2$, and denote the effective width by λ given by $\lambda^2 = \hbar/m_1^*\omega'$, with m_1^* being the effective mass. For $i = 1$ the geometry is shown in detail in Fig. 1(a). Figure 1(b) presents the case $i = 2$. It is assumed that the 2DEG occupies the lowest subband and that it is infinitely thin. As for Fig. 1(c) it shows the geometry for

$i = 3$ with the 3DEG occupying the half-space $z \le -\ell$.

The scattering of one electron gas by another can be characterized by the pertinent relaxation time or frequency. In this paper we consider momentum ν_{1i}^m and energy ν_{1i}^T relaxation frequencies. For their definition we introduce the drift velocities u_i. Following Ref. 14 the friction force between the two gases, R_{1i}, and the power transferred, per particle, from one gas to another, P_{1i}, are given in the linear regime by

$$R_{1i} = m_1^* \nu_{1i}^m (u_1 - u_i), \tag{1}$$

$$P_{1i} = \nu_{1i}^T (T_1 - T_i). \tag{2}$$

These expressions are valid for $|T_1 - T_i| \ll T_1^2/\hbar\tilde{\omega}$, T_1, and $\hbar\tilde{q}(u_1 - u_i) \ll T_1$, where $\tilde{q}$ and $\tilde{\omega}$ are the characteristic values of momentum and energy transfer that occur when one gas is scattered by the other, cf. Ref. 14.

The evaluation of the relaxation frequencies is carried out using the same assumptions as in Ref. 14. Modeling the diagonal part of the density operator with a Fermi-Dirac function whose argument is shifted by $m_1^* u_1$, etc. we obtain, in matrix notation, the following expression:

$$\begin{pmatrix} \nu_{1i}^m \\ \nu_{1i}^T \end{pmatrix} = \frac{2}{\pi^2 n_1} \int_0^\infty \frac{d\omega}{\omega^2} \int_0^\infty dq_x \begin{pmatrix} k_B T_1 q_x^2/m_1^* \\ \omega^2 \end{pmatrix} \frac{\omega_{T_1}}{\sinh(\omega_{T_1})} \frac{\omega_{T_i}}{\sinh(\omega_{T_i})} \mathrm{Im}\Delta\epsilon_1^{\mathrm{eq}}(\omega, q_x)\, \Pi_{1i}(\omega, q_x). \tag{3}$$

Here $\omega_{T_1} = \hbar\omega/2k_B T_1$, $\Delta\epsilon_1^{\mathrm{eq}}(\,)$ is the equilibrium dielectric function of a 1DEG, cf. Refs. 13 and 14. Dropping for simplicity the argument (ω, q_x) we have for the scattering of a 1DEG by a different 1DEG, indicated by $i = 1'$, $\Pi_{11'} = \mathrm{Im}\Delta\epsilon_{1'}^{\mathrm{eq}}/|\epsilon_{11'}|^2$; for the scattering of a 1DEG by a 2DEG ($i = 2$) or by a 3DEG ($i = 3$) the corresponding expression is $\Pi_{1i} = \mathrm{Im}\,\epsilon_s^{(i)}/|\epsilon_s^{(i)} + \Delta\epsilon_1^{\mathrm{eq}}|^2$. The dielectric functions $\epsilon_{11'}$, $\epsilon_s^{(2)}$, and $\epsilon_s^{(3)}$ are calculated in Appendixes A, B, and C, respectively.

Equation (3) has been obtained from the kinetic equation;[14] the latter was derived under the assumption that the electron gases are weakly nonideal and that the interaction between the carriers could be treated by perturbation theory.

An analysis of the integrand in Eq. (3) shows that it is exponentially small for wave vectors q_x and frequencies ω larger than the characteristic values q_c and ω_c, respectively, defined by the following expressions:

$$q_c = \min(k_1, k_i, \ell^{-1}, q_\Lambda), \tag{4}$$

$$\omega_c = \min(k_B T/\hbar, q_c v_1, q_c v_i). \tag{5}$$

Here $T = \min(T_1, T_i)$; $k_i = \sqrt{2m_i^* W_i}/\hbar$ and $v_i = \hbar k_i/m_i^*$ are the thermal or Fermi wave vector and velocity, respectively, and W_i is the mean kinetic energy of the one-, two-, or three-dimensional electron gas. Further, $q_\Lambda = (\epsilon_L/e^2)(m_1^* W_i + m_i^* W_1)/(m_1^* + m_i^*)$ is the Landau wave vector and $1/q_\Lambda$ is the distance where the Coulomb interaction energy between the particles is equal to the sum of their kinetic energies. It is introduced artificially[15,8] to allow for cases where perturbation theory is not valid. The cutoff $k_B T/\hbar$ is easily obtained from the factor $\omega_{T_i}/\sinh(\omega_{T_i})$. The other cutoffs can be obtained from an analysis of the dielectric functions given in the Appendixes.

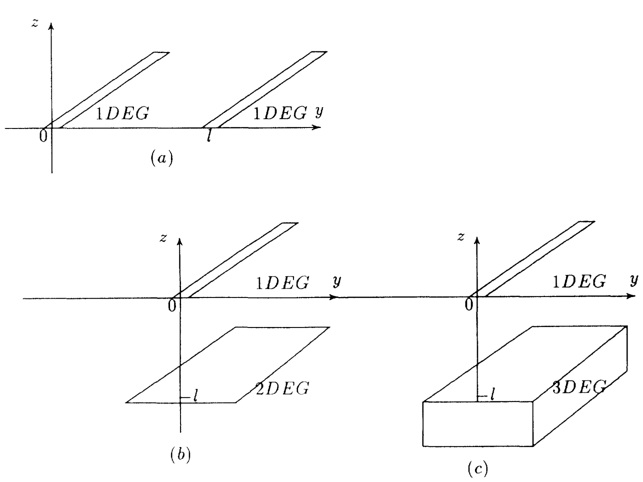

FIG. 1. Geometry. (a) Two 1DEG's, (b) a 1DEG and a 2DEG, (c) a 1DEG and a semibounded 3DEG.

III. ANALYTICAL RESULTS

In this section we present an approximate evaluation of the relaxation frequencies as given by Eq. (3). As a rule, the accuracy of the results is of order unity and logarithmic factors are omitted.

A. Nondegenerate 1DEG

The dielectric function $\Delta\epsilon_1$ of one 1DEG is given approximately by the sum of Eqs. (B5) and (B6) of Ref. 13.

1. Two nondegenerate 1DEG's

For the geometry of Fig. 1(a) we combine the results of Appendix A with that for the dielectric function quoted above and Eq. (3). We then obtain

$$\begin{pmatrix} \nu_{11'}^m \\ \nu_{11'}^T \end{pmatrix} \approx \frac{e^4 n_{1'} \tilde{v}_T}{\epsilon_L^2 v_{T_1} v_{T_{1'}} T_1 T_{1'}} \begin{pmatrix} v_{T_1}^2 \\ \tilde{v}_T^2 \end{pmatrix} \frac{q_c^2}{S(q_c)}. \tag{6}$$

Here $\tilde{v}_T^{-2} = v_{T_1}^{-2} + v_{T_{1'}}^{-2}$ and the factor $S(q_c) \approx [\epsilon_{11'}^s(q_c) + e^2(n_1/T_1 + n_{1'}/T_{1'})]^2/\epsilon_L^2$ describes screening. For weakly nonideal gases the screening is negligible and with logarithmic accuracy we have $S(q_c) \approx 1$.

In two particular cases the frequencies $\nu_{11'}^{m,T}$ can be evaluated more accurately. For $\ell^{-1}, q_\Lambda \gg \tilde{k}_T \equiv (k_{T_1}^{-2} + k_{T_{1'}}^{-2})^{-1/2}$ a more precise result is obtained from Eq. (6) by replacing q_c by $\tilde{k}_T$ and $S(q_c)$ by $\pi^{1/2}[\epsilon_L/\ln \tilde{k}_T^2(\lambda^2 + \lambda'^2)]^2$. The other case is that of large separations between the 1DEG's. When $\ell^{-1} \ll \tilde{k}_T, q_\Lambda$, the cutoff $q \sim \ell^{-1}$ is essential; this results in replacing, in Eq. (6), $q_c^2/S(q_c)$ by $1/\pi^{1/2}\epsilon_L^2\ell^2$.

2. 1DEG scattered by a 2DEG

The geometry is shown in Fig. 1(b). Two cases are important: the first is that of a nondegenerate 2DEG, at high temperatures, or a degenerate 2DEG in the limit $k_BT \gg \hbar v_{12} \min(\ell^{-1}, q_\Lambda)$. Then the cutoff for the integration over ω is $\omega_c \sim q v_{12}$, where $v_{12} = \min(v_{T_1}, v_2)$, and the relaxation frequencies with the help of Appendix B are given by

$$\begin{pmatrix} \nu_{12}^m \\ \nu_{12}^T \end{pmatrix} \approx \frac{e^4 n_2 v_{12}}{\epsilon_L^2 v_{T_1} v_2 T_1 W_2} \left(1 + \frac{q_{2s}}{q_c}\right)^{-2} \begin{pmatrix} v_{T_1}^2 \\ v_{12}^2 \end{pmatrix} \frac{q_c}{S'(q_c)}. \tag{7}$$

The factor $S'(q_x) \approx \{1 + (e^2 n_1/T_1)\mathrm{Re}[1/\epsilon_s^{(2)}(\omega_c, q_x)]\}^2$ introduces screening by the 1DEG and $(1 + q_{2s}/q_c)^{-2}$ that by the 2DEG.

The second case pertains to a degenerate 2DEG in the limit $k_BT \ll \hbar v_{12} \min(\ell^{-1}, q_\Lambda)$ and is opposite to the first one. The cutoff for the ω integration is now $\omega_c \sim k_BT/\hbar$ and the frequencies are given by

$$\begin{pmatrix} \nu_{12}^m \\ \nu_{12}^T \end{pmatrix} \approx \frac{e^4 n_2 v_{T_1}}{\epsilon_L^2 \hbar v_2 W_2} \times \begin{pmatrix} 1/[(1 + q_{2s}/q_c)^2 S'(q_c)] \\ k_{T_1}^2/[(q_{2s} + k_BT/\hbar v_{12})^2 S'(k_BT/\hbar v_{12})] \end{pmatrix}. \tag{8}$$

3. 1DEG scattered by a 3DEG

When $\min(q_c v_{T_1}, q_{3s} v_{T_1}, k_BT/\hbar) \ll \omega_p$ the main contribution to the integral over ω in Eq. (3) comes from the frequencies $\omega \ll \omega_p$. Then using Eq. (C5) we obtain, for arbitrary statistics of the 3DEG, the result

$$\begin{pmatrix} \nu_{13}^m \\ \nu_{13}^T \end{pmatrix} \approx \frac{4\pi e^4 n_3}{\epsilon_L^2 m_1^* v_3 W_3 S'(\tilde{q})} \begin{pmatrix} \tilde{\omega}/\tilde{q} v_{T_1} \\ \tilde{\omega}^3/\tilde{q}^3 v_{T_1}^3 \end{pmatrix} \left(\frac{\tilde{q}}{q_{3s}}\right)^4 \times \left[1 + \ln\left(1 + \frac{q_c}{q_{3s}}\right)\right]. \tag{9}$$

Here $\tilde{q} = \min(q_c, q_{3s})$ and $\tilde{\omega} = \min(\tilde{q} v_{T_1}, k_BT/\hbar)$ are, respectively, the wave vector and frequency that give the largest contributions to the integrals of Eq. (3).

In the opposite limit, $\omega_p \le \min(\tilde{q} v_{T_1}, k_BT/\hbar)$, the main contribution to the integral over ω comes from frequencies close to ω_p, cf. Eqs. (C3)–(C6). The result is given again by Eq. (9) with $\tilde{\omega} = \omega_p$ and $(\tilde{q}/q_{3s})^4$ replaced by $(\tilde{q}/q_{3s})^3$.

As can be seen from Eqs. (6)–(9) at large separations ℓ between the gases the frequencies behave approximately as ℓ^{-2}, ℓ^{-3}, and ℓ^{-4} for scattering by a one-, two-, and three-dimensional electron gas, respectively. On the other hand, at high temperatures, provided that the 1DEG occupies the lowest subband, we have $\nu_{1i}^{m,T} \propto T^{-3/2}$ for all values of i.

Finally, we notice that the cutoff q_c eliminates logarithmic, first-order, and second-order divergencies at high q for scattering by a 3DEG, 2DEG, and 1DEG, respectively.

B. A degenerate 1DEG

For the frequencies $\omega \le k_BT/\hbar$, which give the largest contribution to the integrals in Eq. (3), $\Delta\epsilon_1^{\mathrm{eq}}$ is not exponentially small in two regions. In region A we have $\omega \approx q_x v_{F1}$ and we can write $\mathrm{Im}\Delta\epsilon_{1(A)}^{\mathrm{eq}} \approx (2e^2 q_x/\hbar)\delta(\omega - q_x v_{F1})$ in the numerator of the second line of Eq. (3) while in the denominator we can use the estimate $|\Delta\epsilon_{1(A)}^{\mathrm{eq}}| \approx e^2 m_1^*/\pi\hbar^2 q_x$. In region B we have $q_x \approx 2k_{F_1}$ and, correspondingly, $\mathrm{Im}\Delta\epsilon_{1(B)}^{\mathrm{eq}} \approx (m_1^* e^2\omega/\hbar F_1)\delta(q_x - 2k_{F1})$ and $|\Delta\epsilon_{1,(B)}^{\mathrm{eq}}| \approx (e^2 m_1^*/\pi^2\hbar^2 n_1)\ln(F_1/k_BT_1)$. Here, $k_{F_1} = \pi n_1/2$ and $v_{F_1} = \hbar k_{F_1}/m_1^*$ are the Fermi wave vector and Fermi velocity, respectively. Further details about the dielectric function $\Delta\epsilon_1$ can be found in Appendix B of Ref. 13.

The total relaxation frequencies can be found by adding the two contributions from regions A and B: $\nu^{m,T} = \nu_{(A)}^{m,T} + \nu_{(B)}^{m,T}$; the term (A) is related to small changes in momentum and the term (B) to large momentum changes, i.e., to backscattering of the 1DEG.

1. Scattering by a nondegenerate 1DEG ($i = 1'$)

The result for region A has the form

$$\begin{pmatrix} \nu_{11'}^m \\ \nu_{11'}^T \end{pmatrix}_{(A)} \approx \frac{e^4}{\epsilon_L^2 \hbar v_{F_1} v_{T_{1'}} T_1} \begin{pmatrix} T_{1'}/m_1^* \\ F_1/m_1^* \end{pmatrix} \times e^{-(v_{F1}/v_{T1'})^2} \frac{q_c^2}{S(q_c)}. \tag{10}$$

Here the screening function

$$S(q_x) \approx [1 + (e^2/\epsilon_L)(m_1^*/\pi\hbar^2 q_x + n_{1'}/T_{1'})]^2$$

and can be large for small q_x.

For region B we obtain

$$\begin{pmatrix} \nu_{11'}^m \\ \nu_{11'}^T \end{pmatrix}_{(B)} \approx \frac{e^4}{[\epsilon_{11'}^s(2k_{F_1})]^2 \tilde{S}(2k_{F_1}) v_{F_1} v_{T_{1'}} F_1 T_{1'}} \times \begin{pmatrix} v_{T_{1'}}^2 k_{F_1}^2 \\ \omega_c^2 \end{pmatrix} e^{-(k_{F1}/k_{T1'})^2}\, \Theta(2k_{F_1}/q_\Lambda). \tag{11}$$

Here $\omega_c = \min(k_B T_{1'}/\hbar, 2k_{F_1} v_{T_{1'}})$ and $S(q_x) \approx \{1 + (e^2/\epsilon_L)[(m_1^*/\pi^2\hbar^2 n_1)\ln(F_1/T_1) + n_{1'}/T_{1'}]\}^2$. The function $\Theta(x) \approx 1$ for $x \ll 1$ and is exponentially small for $x \gg 1$. Notice that due to the term $\epsilon^s_{11'}(2k_{F_1})$ this contribution is exponentially small for $\ell \gg 1/2k_{F_1}$, cf. Appendix A.

2. Scattering by a degenerate 1DEG (i =1′)

If the densities of the two gases n_1 and $n_{1'}$ are very different from each other, region A for one gas may overlap with region B of the other. This situation is not realistic; we therefore consider only the case where regions A of both gases are close to each other and assume the same for regions B. If the regions are far from each other we obtain $\nu^{m,T} \propto e^{-F/k_BT}$; these values are very small for strongly degenerate gases.

The first case where the relaxation frequencies are not exponentially small is when $v_{F_1} \approx v_{F_{1'}}$. Then the cutoffs for the q and ω integrals are $q_c = \min(\ell^{-1}, T/\hbar v_{F_1}, q_\Lambda)$ and $\omega_c = q_c v_{F_1}$, respectively. For $T \to 0$ the maximum contribution from regions A is

$$\begin{pmatrix} \nu^m_{11'} \\ \nu^T_{11'} \end{pmatrix}^{\max}_{(A)} \to \frac{\mu e^4}{n_1 \hbar^3 |\epsilon_{11'}(q_c v_{F_1}, q_c)|^2} \begin{pmatrix} k_B T_1/F_1 \\ 1 \end{pmatrix} q_c, \tag{12}$$

where $\mu = m_1^* m_{1'}^*/(m_1^* + m_{1'}^*)$ is the reduced mass and $\epsilon_{11'}$ is given by Eq. (A1) with $|\Delta\epsilon_i(q_c v_{F_i}, q_c)| \approx e^2 m_i^*/\pi\hbar^2 q_c$.

The second case occurs when $k_{F_1} \approx k_{F_{1'}}$, i.e., when the two densities are approximately equal. We then have maximal contribution from the regions B, for $T \to 0$, given by

$$\begin{pmatrix} \nu^m_{11'} \\ \nu^T_{11'} \end{pmatrix}^{\max}_{(B)} \to \frac{\mu m_1^* m_{1'}^* e^4 T}{\epsilon_L^2 \tilde{S}' \hbar^7 n_1^4} \begin{pmatrix} F_1 \\ k_B T_1 \end{pmatrix} e^{-2k_{F_1}\ell} \times\Theta(2k_{F_1}/q_\Lambda), \tag{13}$$

where $\tilde{S}' \approx \{1 + (e^2/\pi^2\epsilon_L\hbar^2 n_1)[m_1^* \ln(F_1/k_BT_1) + m_{1'}^* \ln(F_{1'}/k_BT_{1'})]\}^2$; $\tilde{S}'$ is of order unity for weakly nonideal gases.

3. Scattering by a 2DEG

We consider a 2DEG of arbitrary statistics. Using the results of Appendix B we obtain for region A the result

$$\begin{pmatrix} \nu^m_{12} \\ \nu^T_{12} \end{pmatrix}_{(A)} \approx \frac{e^4 n_2}{\epsilon_L^2 m_1^* F_1 v_2 W_2} \left(1 + \frac{q_{2s}}{q_c}\right)^{-2} \begin{pmatrix} k_B T_1 \\ F_1 \end{pmatrix} \times \frac{q_c}{S'(q_c)}\, \Theta\left(\frac{v_{F_1}}{v_2}\right), \tag{14}$$

with $q_c = \min(\ell^{-1}, k_2, k_BT/\hbar v_{F_1}, q_\Lambda)$. The factors $S'(q_c) \approx \{1 + (e^2 m_1^*/\pi\hbar^2 q_c)\mathrm{Re}[1/\epsilon_s^{(2)}(\omega_c, q_c)]\}^2$ and $(1 + q_{2s}/q_c)^2$ describe the screening by the 1DEG and 2DEG, respectively. The factor $\Theta(v_{F_1}/v_2)$ indicates that the relaxation frequencies are exponentially small for $v_{F_1} \gg v_2$.

For the backscattering contribution we obtain

$$\begin{pmatrix} \nu^m_{12} \\ \nu^T_{12} \end{pmatrix}_{(B)} \approx \frac{e^4 n_2}{\epsilon_L^2 \tilde{S}' v_{F_1} F_1 v_2 W_2 n_1^2} \left(1 + \frac{q_{2s}}{2k_{F_1}}\right)^{-2} \times \begin{pmatrix} k_B T n_1^2/m_1^* \\ \omega_c^2 \end{pmatrix} \omega_c \times\Theta(2k_{F_1}/k_2)\, \Theta(2k_{F_1}\ell)\Theta(2k_{F_1}/q_\Lambda), \tag{15}$$

where

$$\tilde{S}' \approx \{1 + (e^2 n_1/F_1)\ln(F_1/k_BT_1) \times \mathrm{Re}[1/\epsilon_s^{(2)}(k_BT/\hbar, 2k_{F_1})]\}^2.$$

The Θ functions indicate that the result is exponentially small for large separations ℓ, Landau length q_Λ^{-1}, and de Broglie length of the 2DEG k_2^{-1}.

4. Scattering by a 3DEG

We consider a semibounded 3DEG, as indicated in Fig. 1(c), of arbitrary statistics. With the help of Appendix C we find the result [cf. Eq. (9), we omitted for simplicity the logarithmic factor]

$$\begin{pmatrix} \nu^m_{13} \\ \nu^T_{13} \end{pmatrix}_{(A)} \approx \frac{4\pi e^4 n_3}{\epsilon_L^2 S'(\tilde{q}) m_1^* v_3 W_3} \begin{pmatrix} k_B T_1/F_1 \\ 1 \end{pmatrix} \left(\frac{\tilde{q}}{q_{3s}}\right)^4, \tag{16}$$

where $\tilde{q} = \min(q_{3s}, \ell^{-1}, \omega_p/v_{F_1}, k_BT/\hbar v_{F_1}, q_\Lambda)$ is the wave vector that gives the largest contribution to the integral in Eq. (3).

As for the contribution of region B we obtain

$$\begin{pmatrix} \nu^m_{13} \\ \nu^T_{13} \end{pmatrix}_{(A)} \approx \frac{4\pi e^4 n_3}{\epsilon_L^2 S'(\tilde{q}) m_1^* v_3 W_3} \begin{pmatrix} \hbar\tilde{\omega} k_B T_1/F_1^2 \\ (\hbar\tilde{\omega}/F_1)^3 \end{pmatrix} \times \left(\frac{2k_{F_1}}{q_{3s}}\right)^4 \Theta\left(\frac{2k_{F_1}}{q_c}\right). \tag{17}$$

Here the frequency that gives the main contribution to the integral in Eq. (3) is $\tilde{\omega} = \min(k_BT/\hbar, \omega_p, 2k_{F_1}v_3)$.

The analysis given above shows that for a degenerate 1DEG the conservation laws impose strong restrictions on the scattering of the carriers. As a result for small temperatures we have the two distinct regions: A for small momentum changes and B for backscattering, i.e., large momentum changes. For the coupling between two 1DEG's the corresponding contributions to the frequencies will be nonzero if certain relations hold, namely $n_1/m_1^* \approx n_{1'}/m_{1'}^*$ or $n_1 \approx n_{1'}$. For the coupling of a 1DEG with a 2DEG the contribution $\nu^{m,T}_{12(A)}$ survives only if $v_2 \geq v_{F_1}$. These restrictions can be relaxed by considering three-particle interaction, i.e., fourth-order perturbation theory for the scattering.

For large separations between the gases the backscattering contribution is exponentially small and the ℓ dependence of the frequencies is specified by $\nu^{m,T}_{1i(A)}$. Specifically we have $\nu^{m,T}_{13} \propto \ell^{-4}$, $\nu^{m,T}_{12} \propto \ell^{-5}$ (provided $v_2 \geq v_{F_1}$). For the coupling between a degenerate 1DEG and a nondegenerate 1DEG we have $\nu^{m,T}_{11'} \propto \ell^{-4}$ and for two degenerate 1DEG's $\nu^{m,T}_{11'} \propto \ell^{-3}$ provided $n_1/m_1^* \approx n_{1'}/m_{1'}^*$.

As for the temperature dependence we have the following results for low temperatures: $\nu^{m,T}_{12(B)} \propto \nu^{m,T}_{13(B)} \propto T^{2,3}$ $\nu^{m,T}_{12(A)} \propto T^{6,5}$, and $\nu^{m,T}_{13(A)} \propto T^{7,6}$; the first exponent in T is for momentum and the second one for temperature relaxation. Thus, for moderate separations (when the contribution of region B is not negligible) and low temperatures the main contribution is due to backscattering. We also notice that the inequality $\nu^m < \nu^T$ is possible for degenerate gases: it means that the temperature (*not energy*) relaxation is more rapid than the momentum relaxation.

IV. NUMERICAL CALCULATIONS

To support our analytical results we have performed numerical calculations of relaxation frequencies in several interesting cases of coupling between *degenerate* electron gases of the same or different dimensionality as well as between a 1DEG and a 1D hole gas. We used Eq.(3) together with the results of Appendixes A, B, and C. For the imaginary part of $\Delta\epsilon_1^{\rm eq}(\omega, q_x)$ we took the exact expression (B3) of Ref. 13 valid for arbitrary statistics of the 1DEG. As for the real part of $\Delta\epsilon_1^{\rm eq}(\omega, q_x)$ and the dielectric functions of the 2DEG and 3DEG we used the results for the strongly degenerate limit, see Refs. 11 and 3.

For the sake of concreteness, we have chosen the confining potential in y direction to be parabolic with an effective width $\lambda = 90$ Å, while the thickness in the z direction was taken to be zero. It should be mentioned that for one subband occupation (as in this paper) the form of the confining potential affects the result very little and only quantitatively. We also chose parameters pertinent to a GaAs/Al$_x$Ga$_{1-x}$As heterostructure: dielectric constant $\epsilon_L = 13$; effective mass: $m_e^* = 0.067m_0$ for electrons and $m_h^* = 0.37m_0$ for holes.

In Figs. 2, 3, and 4 we present the results of calculations for mutual scattering between a *degenerate* 1D *electron* and a 1D *hole* gas. As was stated in Sec. III B at sufficiently low temperature due to the strong restrictions imposed on the scattering, in one dimension, by the momentum and energy conservation laws as well as by the Pauli principle, only two sorts of processes are allowed.

One of them is backscattering, i.e., the large change of carrier momentum equal to $\hbar q_x \approx 2\hbar k_F$, or region B in the ω-q_x plane. For mutual scattering of *strongly* degenerate 1D gases the contribution of backscattering to the relaxation frequencies is not exponentially small if the concentrations of the gases are approximately equal [see Eq. (13)]. Figure 2 illustrates this statement for scattering between degenerate electron-and-hole gases. The hole concentration is $n_h = 10^6$ cm^{-1}, the distance between the gases is taken to be zero. At $T = 1$ K the peak at $n_e = n_h$ is clearly seen; at higher temperatures it is smeared out. The increase of $\nu^{m,T}_{eh}$ with decreasing n_e at $T = 10$ K is related to the weakening of degeneracy and the increase in the number of allowed transitions in k space.

The second possible scattering process in strongly degenerate 1DEG's is small momentum change, namely $\hbar q_x \approx \hbar\omega/v_F \ll 2\hbar k_F$ (region A). As follows from the analysis in Sec. III B [see Eq. (12)], at sufficiently low temperatures the contribution of processes with small momentum change to scattering between two 1D gases is not exponentially small if their Fermi velocities are equal. This is illustrated in Fig. 3. The parameters are the same as in Fig. 2. For $T \leq 1$ K the peak at $n_e \approx n_h m_e/m_h \approx 1.7\times10^5$ cm^{-1} (i.e., $v_{Fe} \approx v_{Fh}$) is seen clearly; at higher temperatures it is smeared out.

We should mention that when backscattering processes

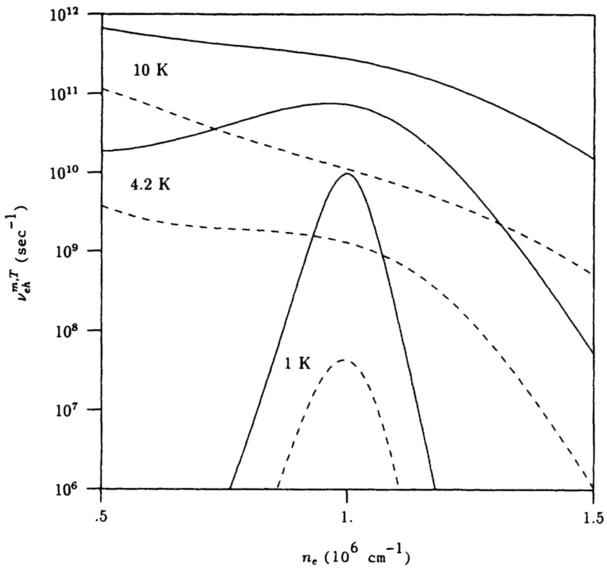

FIG. 2. Momentum (solid line) and temperature (dashed) relaxation frequencies vs electron concentration for a 1DEG scattered by a 1D hole gas. Separation between gases $\ell = 0$; hole concentration $n_h = 10^6$ cm^{-1}; temperature $T = 1, 4.2, 10$ K. The maximum occurs at $n_e \approx n_h$.

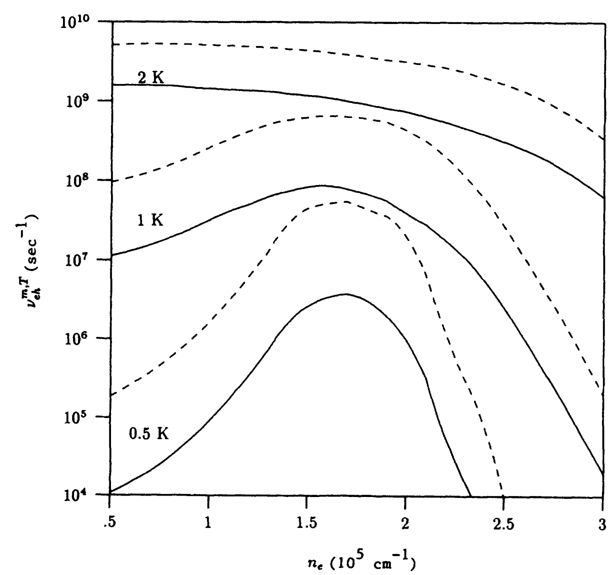

FIG. 3. The same as in Fig. 2. Temperature $T = 0.5, 1, 2$ K. The maximum occurs at $v_{Fe} \approx v_{Fh}$.

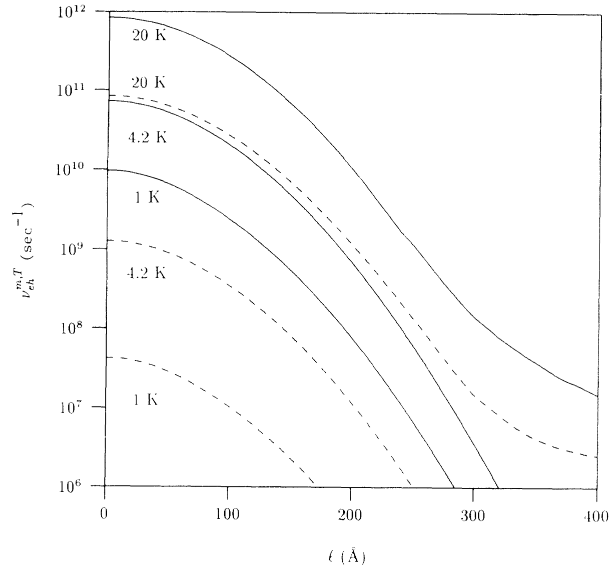

FIG. 4. 1D electron gas scattered by 1D hole gas. Momentum (solid) and temperature (dashed) relaxation frequencies vs distance between the gases. Temperature $T = 1, 4.2, 10$ K; concentrations $n_e = n_h = 10^6$ cm^{-1}.

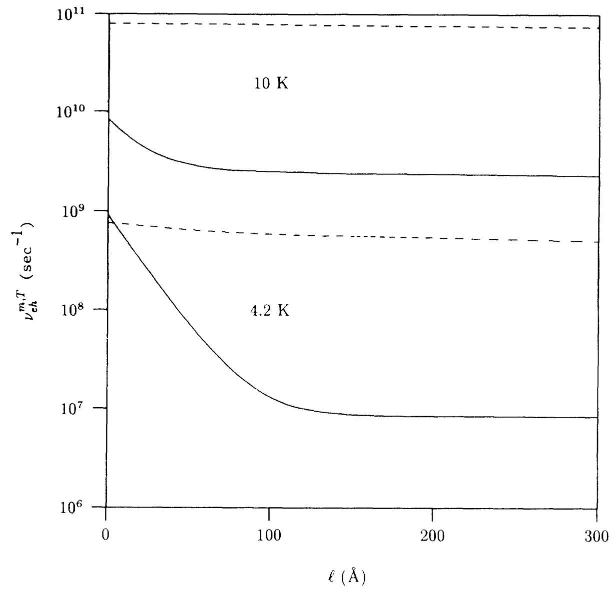

FIG. 5. 1DEG scattered by 2DEG. Momentum (solid) and temperature (dashed) relaxation frequencies vs distance between the gases. Concentrations $n_1 = 8 \times 10^5$ cm^{-1}, $n_2 = 5 \times 10^{11}$ cm^{-2}; temperature $T = 4.2, 10$ K.

dominate (Fig. 2) the temperature relaxation frequency (dashed lines) is smaller than the momentum relaxation frequency (solid lines); the reverse holds when region A dominates, cf. Fig. 3. The reason is that at backscattering the momentum change is large ($\hbar q_x \approx 2\hbar k_F$), while the change in energy ($\hbar\omega \sim k_B T \ll F$) is relatively small. The processes with small change of momentum still have strong influence on the form of the distribution function at $k \approx \pm k_F$. Thus, in the degenerate case the rate of *temperature* relaxation can be much larger than that of *energy* relaxation.

Notice that in accordance with Eqs. (12) and (13) the difference between ν^m and ν^T is larger for lower temperatures. In fact, Eq. (13) implies $\nu_{(B)}^m/\nu_{(B)}^T \propto F/k_BT$ for the contribution of backscattering, and Eq. (12) gives $\nu_{(A)}^T/\nu_{(A)}^m \propto F/k_BT$ for small momentum changes.

Figure 4 illustrates the dependence of the relaxation frequencies on the distance between the gases. The concentrations of electron-and-hole gases are equal, and therefore the backscattering contribution dominates. We see that the relaxation frequencies decrease exponentially with ℓ when the separation between the gases is greater than the inverse de Broglie length $k_F^{-1} \approx 60$ Å [cf. factor $e^{-2k_{F1}\ell}$ in Eq. (13)]. For $T = 20$ K and $\ell \geq 300$ Å the contribution of processes other than backscattering becomes essential.

In Figs. 5 and 6 we present the results of numerical calculations for a 1D electron gas scattered by a 2D electron gas. In Fig. 5 we plot the momentum and energy relaxation frequencies $\nu_{13}^{m,T}$ versus distance ℓ between the gases; the 1D and 2D carrier concentrations are, respectively, $n_1 = 8 \times 10^5$ cm^{-1} and $n_2 = 5 \times 10^{11}$ cm^{-2}. At small ℓ the *momentum* relaxation frequencies are specified mainly by backscattering processes, and the scattering rate decreases exponentially with ℓ in accordance with Eq. (15). At larger separations between the gases the contribution of region A dominates and for $\ell < \hbar v_{F_1}/k_BT$ the relaxation frequencies depend very weakly on ℓ, cf. Eq. (14). As for the *temperature* relaxation frequency, the contribution of region B is always small in comparison with that of A, and the dependence on ℓ is weak.

Figure 6 shows the relaxation frequencies as a func-

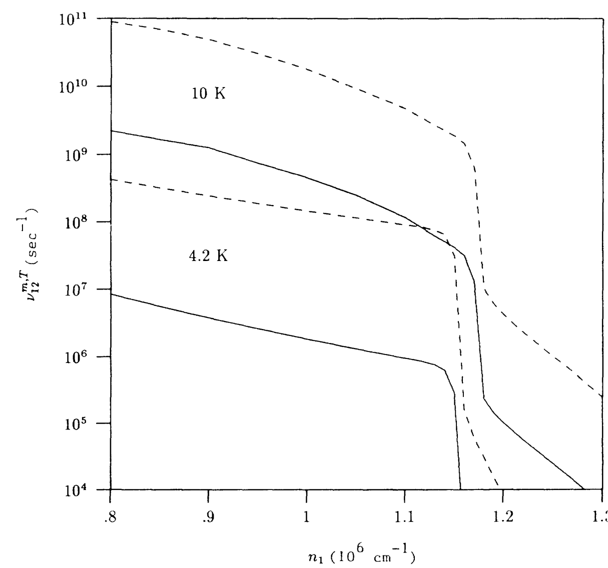

FIG. 6. 1DEG scattered by 2DEG. Momentum (solid) and temperature (dashed) relaxation frequencies vs 1DEG concentration. Distance between the gases $\ell = 300$ Å; 2DEG concentration $n_2 = 5 \times 10^{11}$ cm^{-2}; temperature $T = 4.2, 10$ K.

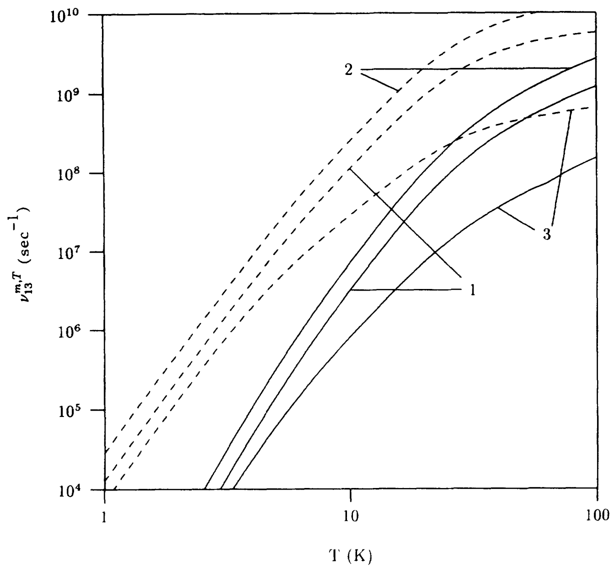

FIG. 7. A 1DEG scattered by a semibounded 3DEG. Momentum (solid) and temperature (dashed) relaxation frequencies vs temperature. The 1DEG concentration is $n_1 = 10^6$ cm^{-1}. Curves 1: $\ell = 300$ Å, $n_3 = 10^{18}$ cm^{-3}; curves 2: $\ell = 300$ Å, $n_3 = 3\times10^{17}$ cm^{-3}; curves 3: $\ell = 600$ Å, $n_3 = 10^{18}$ cm^{-3}.

tion of the 1DEG concentration; the distance between the gases $\ell = 300$ Å, the concentration of 2DEG is $n_2 = 8 \times 10^{11}$ cm^{-2}. Since the separation between the gases is much larger than the inverse de Broglie length, the contribution of backscattering is negligible [cf. the factor $\Theta(2k_{F_1}\ell)$ in Eq. (14)] and the relaxation is determined by the contribution of region A. In accordance with the factor $\Theta(v_{F_1}/v_2)$ in Eq. (14), a sharp decrease in coupling between the gases occurs at $n_1 > \sqrt{8n_2/\pi} \approx 1.13 \times 10^6$ cm^{-1}, i.e., for $v_{F_1} > v_{F_2}$. The reason is that in the degenerate limit and for large separations between the gases only transitions with $\omega \approx q_x v_{F_2}$ can occur in the 1DEG, while for the 2D carriers the processes with $\omega \leq q_x v_{F_2}$ are allowed. Thus, for $v_{F_1} \geq v_{F_2}$ the coupling between the gases becomes exponentially small.

Figure 7 shows the results for scattering of a 1DEG by a semibounded 3DEG. The relaxation frequencies are plotted as function of the temperature for different values of ℓ and n_3 (see caption); the 1DEG concentration is $n_1 = 10^6$ cm^{-1}. For distances $\ell = 300$ and 600 Å used in the calculations only the contribution of region A is essential. At $T < 30$ K we have approximately $\nu_{13}^m \propto T^5$ and $\nu_{13}^T \propto T^4$ in accordance with Eq. (16) with $\tilde{q} = k_B T/\hbar v_{F_1} < e^2 m_1^*/\pi\hbar^2\epsilon_L$. At higher temperatures (provided that the gases are degenerate) the cutoff $q \sim \ell^{-1}$ is essential and we have $\nu_{13}^m \propto T$, $\nu_{13}^T \propto T^0$ take place. Notice that the relaxation frequencies for $n_3 = 3 \times 10^{17}$ cm^{-3} (curves 2) are larger than those for $n_3 = 10^{18}$ cm^{-3} (curves 1) due to the stronger screening in the 3DEG when the concentration is higher.

We should mention that in Figs. 3–7, where the contribution of small momentum changes dominates, one can see that $\nu^m/\nu^T \sim k_B T_1/F_1$ in accordance with Eqs. (12), (14), and (16).

V. DISCUSSION

In this article we made analytical evaluations and numerical calculations of the momentum and temperature relaxation frequencies for a 1DEG scattered by (a) another 1DEG or a 1D hole gas, (b) a 2DEG, and (c) a semibounded 3DEG. The calculations were based on Eq. (3) derived previously[14] with the relevant dielectric functions presented in the Appendixes. The gases are separated by a distance ℓ and have the same or different statistics; moreover, dynamic screening has been taken into account.

We found that for *nondegenerate* gases the cutoff $q \sim q_c$ [cf. Eq. (4)] eliminates logarithmic, first-, and second-order divergencies in the integration over q_x for a 1DEG scattered by 3D, 2D, and 1D carriers, respectively. It should be compared to the elimination of the logarithmic divergence for scattering of a 3DEG by a 3DEG (Ref. 15) or a 2DEG (Ref. 11) and first-order divergence for mutual scattering of two 2D gases. At large distance ℓ between the gases, as follows from Eqs. (6)–(9), the relaxation frequencies are proportional to ℓ^{-1-i} for a 1DEG scattered by an i-dimensional electron gas ($i = 1,2,3$). At high temperatures we have $\nu_{1i}^{m,T} \propto T^{-3/2}$ for all dimensionalities.

For *strongly degenerate* 1DEG's the restrictions imposed on the scattering by the conservation laws and the Pauli principle forbid all transitions in k_x space except two types: one with small momentum changes, $q_x \approx \omega/v_{F_1} \ll k_{F_1}$ (region A), and one due to backscattering, $q_x \approx 2k_{F_1}$ (region B). The contribution of backscattering is exponentially small for small cutoff wave vector q_c; therefore at large separations ℓ between the gases only the contribution of region A is essential.

As for the scattering of two strongly degenerate 1D gases the coupling is not exponentially small only if the regions B or A of both gases overlap, that is if $n_1 \approx n_{1'}$ or $v_{F_1} \approx v_{F_{1'}}$ (cf. Figs. 2 and 3). Moreover, the scattering of a 1DEG by a 2DEG is not small if $v_{F_1} < v_2$ (cf. Fig. 6). The restrictions due to the conservation laws can be relaxed by taking into account three-particle interactions in higher orders of perturbation theory.

We should mention that when the contribution of small momentum changes to the relaxation frequencies is dominant, *temperature* (not energy) relaxation in degenerate gases is faster than that of momentum. In fact, as follows from Eqs. (12), (14), and (16) $\nu_{(A)}^m/\nu_{(A)}^T \sim k_B T_1/F_1$ for all dimensionalities of the gases.

It is worth noticing that the screening by carriers of a *nondegenerate* 1DEG cannot be strong provided that the gas is weakly nonideal (an implicit assumption usually made in derivations of kinetic equations); the same situation occurs for scattering of a 1DEG of arbitrary statistics by a *static* potential. This statement is no longer valid for the screening of a degenerate 1DEG interacting with another electron gas. When $q_c \leq e^2 m_1^*/\pi\hbar^2\epsilon_L$ and $\omega_c \sim q_c v_{F_1}$ (e.g., at large distances between the gases) the screening by the 1DEG can be essential.

ACKNOWLEDGMENTS

The work of one of us (P.V.) was supported by NSERC Grant No. URF0116877. We thank Dr. H. C. Tso for help in part of the computer work.

APPENDIX A

The screening function for interaction between 1DEG's is given by Eq. (25) of Ref. 14. For two sorts of carriers occupying the lowest subband it takes the form

$$\epsilon_{11'} = \epsilon^s_{11'}\left[1 + \frac{\Delta\epsilon_1}{\epsilon^s_{11}} + \frac{\Delta\epsilon_{1'}}{\epsilon^s_{1'1'}} + \Delta\epsilon_1\Delta\epsilon_{1'}\left(\frac{1}{\epsilon^s_{11}\epsilon^s_{1'1'}} - \frac{1}{\epsilon^s_{11'}\epsilon^s_{1'1}}\right)\right], \tag{A1}$$

where we have dropped the argument (ω, q_x) for simplicity. The dielectric functions of the external system, indicated by the superscript s, are specified by the geometry of the latter and the wave functions of the carriers in the transverse direction, cf. Eq. (21) of Ref. 14.

For the geometry of Fig. 1(a), with a parabolic confinement in the y direction and zero thickness, Eqs. (11), (19), and (27) of Ref. 13 yield

$$\frac{1}{\epsilon^s_{11}} = \frac{1}{\epsilon_L}\, e^{(\lambda q_x/2)^2} K_0[(\lambda q_x/2)^2], \tag{A2}$$

$$\frac{1}{\epsilon^s_{11'}} = \frac{2}{\epsilon_L}\int_0^\infty \frac{dq_y}{\sqrt{q_x^2 + q_y^2}} \cos(q_y\ell)\, e^{-\bar\lambda^2 q_y^2/2}. \tag{A3}$$

Here $2\bar\lambda^2 = \lambda^2 + \lambda'^2$ and $K_0(z)$ is the modified Bessel function. The expression for $1/\epsilon^s_{1'1'}$ can be obtained from Eq. (A2) with 1 and λ replaced by $1'$ and λ', respectively.

An important limit of the last two expressions is obtained for $q_x\lambda \ll 1$ (notice that for a 1DEG occupying the lowest subband we always have $q_x\lambda \le 1$). Then $1/\epsilon^s_{11} \approx (2/\epsilon_L)\ln(1/\lambda q_x)$. As for $1/\epsilon^s_{11'}$ it is equal to $(1/\epsilon_L)\ln[q_x^{-2}(\bar\lambda^2 + \ell^2)^{-1}]$ if $q_x\ell \ll 1$ and to $(1/\epsilon_L)\sqrt{2\pi/q_x\ell}\, e^{-q_x\ell}$ for $q_x\ell \gg 1$.

For finite thickness (along the z axis) and a square-confining potential in the y direction the corresponding expressions can easily be worked out with the help of Eqs. (16)–(20), (22), (30), and (32) of Ref. 13.

APPENDIX B

Below we evaluate the dielectric function pertinent to the geometry of Fig. 1(b). Using Eqs. (27) and (19) of Ref. 13 we can write

$$\frac{1}{\epsilon_s(\omega, q_x)} = 2e^{\lambda^2 q_x^2/2}\int_{q_x}^\infty \frac{e^{-\lambda^2 k^2/2}dk}{\epsilon_s(\omega, k)\sqrt{k^2 - q_x^2}}, \tag{B1}$$

where $\mathbf{k} = (q_x, q_y)$; the dielectric function $\epsilon_s(\omega, k)$ is defined by Eq. (28) of Ref. 13. For an infinitely thin layer of 1DEG we obtain

$$\epsilon_s(\omega, k) = \frac{\epsilon_L}{2}\left[1 + \frac{\beta(\omega, k)\tanh(k\ell) + 1}{\beta(\omega, k) + \tanh(k\ell)}\right]. \tag{B2}$$

The function $\beta(\omega, k)$, specified by the boundary condition on the electrostatic potential at $z = -\ell$, is given by Eq. (29) of Ref. 13.

Matching the solutions of Poisson's equation in all regions of Fig. 1(b) we obtain, for an infinitely thin 2DEG,

$$\beta^{(2)}(\omega, k) = \frac{\epsilon_L}{\epsilon_L + 2\Delta\epsilon_2(\omega, k)}. \tag{B3}$$

From the previous three equations and the function $\Delta\epsilon_2(\omega, k)$, defined in Refs. 3 and 11, we can estimate, with accuracy of the order of unity, the function $1/\epsilon^{(2)}_s(\omega, q_x)$. Its real part is equal to $1/\epsilon_L$ everywhere except for $q_{2s} \ll q_x \ll 1/\ell$ in which case it is equal to $q_{2s}/q_x\epsilon_L$, where $q_{2s} = 2\pi e^2 n_2/\epsilon_L W_2$ is the screening wave vector of the 2DEG and $W_2 = \min(T_2, F_2)$ is the thermal or Fermi velocity.

For the imaginary part the result is

$$\mathrm{Im}\frac{1}{\epsilon^{(2)}_s} \approx \frac{\omega q_{2s} G}{\epsilon_L v_2\,(q_x + q_{2s})^2}\,\frac{e^{-2q_x\ell}}{1 + \sqrt{q_x(\ell + \lambda)}} \times\Theta(q_x v_2/\omega)\,\Theta(k_2/q_x). \tag{B4}$$

We have $G = 1$ when the 2DEG is degenerate and $G = \sinh(\hbar\omega/2k_B T_2)/(\hbar\omega/2k_B T_2)$ when it is nondegenerate.

APPENDIX C

Below we calculate the dielectric function $1/\epsilon^{(3)}_s(\omega, q_x)$ pertinent to the geometry of Fig. 1(c). It is given by Eqs. (B1) and (B2) after specifying the function $\beta^{(3)}(\omega, q_x)$ for the 3DEG.

Assuming specular reflection of the carriers at the boundary $z = -\ell$ and a homogeneous 3DEG for $z < \ell$ the function $\beta^{(3)}$ is given by Eqs. (A3)–(A9) of Ref. 3. For an approximate calculation we split this function in a plasmon contribution β_{pl} and a regular contribution β_{reg}. The first one is nonzero only for $q \ll q_{3s}$ where q_{3s} is the screening wave vector of an unbounded 3DEG. Its value is

$$\beta^{(3)}_{\mathrm{pl}} \approx \omega^2/[(\omega - \omega_p + i0)(\omega + \omega_p + i0)], \tag{C1}$$

where $\omega_p = \sqrt{4\pi e^2 n_3/\epsilon_L m_3^*}$ is the plasma frequency. As for the regular contribution we obtain

$$\beta^{(3)}_{\mathrm{reg}} \approx \frac{qv_3}{\omega + \omega_p + qv_3} - i\frac{\omega\omega_p^2 qv_3}{\omega^4 + \omega_p^4 + (qv_3)^4}. \tag{C2}$$

Using Eqs. (B1), (B2), and (C2) we can estimate the function $1/\epsilon^{(3)}_s$. Its real part is everywhere approximately equal to $1/\epsilon_L$, except in the following two cases: (i) for $\omega \ll \omega_p$, $q_x\ell \ll 1$, and $q_{3s}\lambda \gg 1$ it is much smaller than $1/\epsilon_L$; (ii) for $\omega \approx \omega_p/\sqrt{2}$, $q \ll q_{3s}$ it is about $\omega_p/(\omega - \omega_p/\sqrt{2})$.

As for the imaginary part we split it in plasmon and regular parts. The first part is nonzero only for $q_x \ll q_{3s}$; it is given by

$$\mathrm{Im}\frac{1}{\epsilon^{(3)}_{s,\mathrm{pl}}} \approx \omega_p\,\delta(\omega - \omega_p/\sqrt{2})A, \tag{C3}$$

where $A = \epsilon_L^{-1} e^{-2q_x\ell}\Theta(q_x/q_{3s})/[1+\sqrt{q_x\ell+q_x\lambda}]$.

For the regular part we have the following asymptotic results:

$$\mathrm{Im}\frac{1}{\epsilon_{s,\mathrm{reg}}^{(3)}} \approx \frac{\omega q_x v_3}{\omega_p^2} A, \quad \omega, q_x v_3 \ll \omega_p, \tag{C4}$$

$$\mathrm{Im}\frac{1}{\epsilon_{s,\mathrm{reg}}^{(3)}} \approx \frac{\omega q_{3s}^2}{q_x^3 v_3} A, \quad \omega, \omega_p \ll q_x v_3, \tag{C5}$$

$$\mathrm{Im}\frac{1}{\epsilon_{s,\mathrm{reg}}^{(3)}} \approx (\omega_p^2 v_3/\omega^3)\min[(\ell+\lambda)^{-1}, \omega/v_3]A, \quad \omega_p, q_x v_3 \ll \omega. \tag{C6}$$

All expressions of this appendix are valid for a classical description of a 3DEG. To allow for a quantum description the last four expressions must be multiplied by a factor $\Theta(q_x/k_3)$.

[1] P. J. Price, Physica **117B**, 750 (1983); C. Jacoboni and P. J. Price, Solid State Electron. **31**, 649 (1988).

[2] I. I. Boiko and Yu. M. Sirenko, Zh. Tekh. Fiz. **33**, 967 (1988) [Sov. Phys. Tech. Phys. **33**, 586 (1988)].

[3] I. I. Boiko and Yu. M. Sirenko, Phys. Status Solidi B **159**, 805 (1990).

[4] P. M. Solomon, J. Price, D. J. H. Frank, and D. C. La Tulipe, Phys. Rev. Lett. **63**, 2508 (1989).

[5] T. J. Gramila, J. Eisenstein, A. H. MacDonald, L. N. Pfeiffer, and K. W. West, Phys. Rev. Lett. **66**, 1216 (1991).

[6] T. J. Gramila, J. Eisenstein, A. H. MacDonald, L. N. Pfeiffer and K. W. West, Surf. Sci. (to be published).

[7] B. Laikhtman and P. Solomon, Phys. Rev. B **41**, 9921 (1990); D. L. Maslov, *ibid.* **45**, 1911 (1992).

[8] I. I. Boiko, P. Vasilopoulos, and Yu. M. Sirenko, Phys. Rev. B **45**, 13 538 (1992).

[9] H. C. Tso, P. Vasilopoulos, and F. M. Peeters, Phys. Rev. Lett. **68**, 2516 (1992).

[10] H. C. Tso and P. Vasilopoulos, Phys. Rev. B **45**, 1333 (1992); Surf. Sci. **263**, 368 (1992).

[11] I. I. Boiko and Yu. M. Sirenko, Ukr. Fiz. Zh. (Ukr. Ed.) **34**, 1071 (1991).

[12] P. Vasilopoulos and H. C. Tso, *Proceedings of the CAPNSERC Workshop on Excitations in Superlattices and Multi-Quantum Wells* (Springer-Verlag, London, 1991).

[13] I. I. Boiko, Yu. M. Sirenko, and P. Vasilopoulos, Phys. Rev. B **43**, 7224 (1991).

[14] I. I. Boiko, Yu. M. Sirenko, and P. Vasilopoulos, Phys. Rev. B **43**, 7216 (1991).

[15] Yu. L. Klimontovich, *Statistical Physics* (Harwood Academic, New York, 1986).